

**Violation of Bell inequalities and
Quantum Tomography with
Pure-states, Werner-states and
Maximally Entangled Mixed States
created by a Universal Quantum Entangler**

M. Barbieri, F. De Martini, G. Di Nepi and P. Mataloni

Dipartimento di Fisica and

Istituto Nazionale per la Fisica della Materia

Università di Roma "La Sapienza", Roma, 00185 - Italy

Abstract

Entangled pure-states, Werner-states and generalized mixed-states of any structure, spanning a 2×2 Hilbert space are created by a novel high-brilliance universal source of polarization-entangled photon pairs. The violation of a Bell inequality has been tested for the first time with a *pure-state*, indeed a conceptually relevant *ideal* condition, and with Werner-states. The generalized "maximally entangled mixed states" (MEMS) were also synthesized for the first time and their exotic properties investigated by means of a quantum tomographic technique. PACS numbers: 03.67.Mn, 03.65.Ta, 03.65.Ud, 03.65.Wj

Entanglement, "*the characteristic trait of quantum mechanics*" according to Erwin Schroedinger, is playing an increasing role in nowadays physics [1]. Indeed it is the irrevocable signature of quantum nonlocality, i.e. the scientific paradigm today recognized as the fundamental cornerstone of our, yet uncertain understanding of the Universe. The striking key process, the "*bolt from the blue*" [i.e. from the skies of Copenhagen] according to Leo Rosenfeld [2], was of course the EPR discovery in 1935 followed by a much debated endeavour ended, in the last few decades by the lucky emergence of the Bell's inequalities and by their crucial experimental verification [3]. In the last years the violation of these inequalities has been tested so many times by optical experiments that (almost) no one today challenges the reality of quantum nonlocality. However, there still exist few crucial "loop-holes" of experimental nature that have not been adequately resolved. As far as optical experiments is concerned, the most important one is the *quantum-efficiency* "loophole" that refers to the lack of detection of *all couples* of entangled photons which can be generated by the EPR source within any elementary QED creation process. This effect can be due both to the limited efficiency of the detectors [4] and to the loss of the created pairs that for geometrical reasons do not reach the detectors. While the first contribution, expressed by the *detector quantum efficiency* (DQE) can be attain 50% or more, the second most important contribution, the *source quantum efficiency* (SQE), has been of the order 10^{-4} or less in all EPR experiments performed thus far. For instance, in all Spontaneous Parametric Down Conversion (SPDC) experiments the test photon pair was filtered by two narrow pinholes out of a very wide \vec{k} - *vector* distribution spatially emitted, for any common λ of the emitted particles, over one or two cones, depending on the physical orientation of the nonlinear crystal [5]. In other words, the *detected* photon pairs in *all* Bell inequalities tests, indeed *statistical* experiments, were in a highly *mixed-state*, implying that the ensemble joint detection probabilities related to the *emitted* particles were not directly accessible to measurement. The lack of detection efficiency and the *lack of purity* of the state of the tested pairs were of deep concern to John Bell himself [6] and required the adoption of reasonable *supplementary assumptions* such as "*fair sampling*" [7] and "*no-enhancement*"

[8] within any acceptable interpretation of the results.

On the other hand, in modern Quantum Information (QI) the quest for the conceptually appealing *pure-states* is somewhat counterbalanced, for *practical* reasons, by the increasing emergence of the *mixed-states* in the real world. Because of the unavoidable effects of the decohering interactions indeed these states are today considered the basic constituents of modern QI and Quantum Computation as they limit the performance of all quantum communication protocols including *quantum dense coding* [9] and *quantum-state teleportation* (QST) [10]. It is not surprising that in the last few years, within an endeavour aimed at the use of *mixed-states* as a practical *resource*, an entire new branch of arduous mathematics and topology has been created to investigate the quite unexplored theory of the *positive-maps* (*P-maps*) in Hilbert spaces in view of the assessment of the "*residual entanglement*" and of the establishment of more general "*state-separability*" criteria [11]. Very recently this ambitious study has reached results that are conceptually relevant, as for instance the discovery of a *discontinuity* in the structure of the *mixed-state* entanglement. Precisely, the identification of two classes: the *free-entanglement*, useful for quantum communication, and the *bound-entanglement*, a *non-distillable* mysterious process, elicited a fascinating new horizon implied by the basic question: what is the role of *bound* entanglement in Nature [12] ?

Since any real advancement in modern physics cannot be attained without parallel, mutually testing and inspiring, experimental and theoretical endeavours, it appears evident the present need in QI of a universal, flexible source by which entangled *pure-* as well *mixed-states* of any structure could be easily engineered in a reliable and reproducible way. In the present work we present a nonlinear (NL) optical SPDC source that indeed possesses these properties. Another lucky structural property of this source is the very *high-brilliance*, order of magnitude larger than the conventional ones. Consistently with the above considerations, in the present work this source will be applied to two different, somewhat "extreme" experiments, both implying a bi-partite, two qubit entangled state. A first experiment will consist of the first Bell inequality violation experiment involving a

pure-state, $SQE \approx 1$, i.e. by which *all* the SPDC generated photon pairs are allowed to excite the cathode of the testing detectors. By a second experiment, the same inequality will be tested by several Werner *transition-mixed-states*, i.e. belonging to a set for which the violation is theoretically expected to be zero [13]. In addition, a quantum tomographic analysis will be then undertaken of the Werner states with variable mixing parameters. At last, the highly relevant "*maximally entangled mixed states*" (MEMS), today of common interest, will be created and tested by the same technique [14]. All these states have been easily synthesized by our source for the first time, to the best of our knowledge.

Let us give here a detailed description of the apparatus. A slab of β -barium-borate (BBO) NL crystal, .5mm thick and cut for Type I phase-matching, was excited by a vertically (V) polarized, slightly focused, cw UV Ar^+ laser beam ($\lambda_p = 363.8nm$) with wavevector (wv) $-\mathbf{k}_p$, i.e. directed towards the left-hand-side (lhs) of Fig.1. In our experiment the investigated NL interaction was λ -degenerate, i.e. the photons of each SPDC generated i^{th} -pair had *equal* wavelengths (wl) $\lambda = \lambda_{ji} = 727.6nm$, ($j = 1, 2$), common horizontal (H) linear-polarization ($\vec{\pi}$), and were emitted with *equal probability*, over a corresponding pair of wavevectors (wv) \mathbf{k}_{ji} belonging to the surface of a cone with axis \mathbf{k}_p and aperture $\alpha \simeq 2.9^\circ$. The *product-state* of each emitted i^{th} -pair was expressed as: $|\Phi\rangle_i = |HH\rangle_i$, where the shorthand: $|XY\rangle \equiv |X\rangle \otimes |Y\rangle$ is and will be used henceforth. The emitted radiation and the UV laser beam directed towards the lhs of Fig.1 were then back-reflected by a multilayer-dielectric spherical mirror M with curvature radius $R = 15cm$, highly reflecting ($\approx 99\%$) both λ and λ_p , placed at a distance $d = R$ from the crystal. A zero-order $\lambda/4$ waveplate (wp) placed between M and the NL crystal, i.e. in the " $d - section$ ", as we call it, intercepted twice both back-reflected λ and λ_p beams and then rotated by 90° the polarization ($\vec{\pi}$) of the back-reflected photons with wl λ while leaving in its original $\vec{\pi}$ state the back-reflected UV beam $\lambda_p \approx 2\lambda_j$. In facts, it has been verified that the $\lambda/4$ wp acted closely as a $\lambda_p/2$ wp. The back-reflected UV beam excited in the direction \mathbf{k}_p an identical albeit distinct SPDC process with emission of a new radiation cone directed towards the (rhs) of Fig.1 with axis \mathbf{k}_p . In this way each i^{th} -pair of correlated vw's, \mathbf{k}_{ji} ($j=1,2$) originally

SPDC generated towards the lhs of Fig. 1 was made, by optical back-reflection and a unitary $\vec{\pi}$ -flipping transformation, "in principle indistinguishable", i.e. for any *ideal* detector placed in \mathcal{A} and/or \mathcal{B} , with another pair originally generated towards the rhs and carrying the state $|HH\rangle_i$. In virtue of the quantum superposition principle, the state of the overall radiation, resulting from the overlapping of the two *indistinguishable* cones expressing the corresponding overall \mathbf{k}_{ji} -distributions, was then expressed by the *pure-state*:

$$|\Phi\rangle = 2^{-\frac{1}{2}} (|HH\rangle + e^{i\phi}|VV\rangle) \quad (1)$$

an entangled Bell-state, with a phase ($0 \leq \phi \leq \pi$) reliably controlled by micrometric displacements Δd of M along \mathbf{k}_p . A positive lens with focal-length F transformed the overall emission *conical* distribution into a *cylindrical* one with axis \mathbf{k}_p . The transverse circular section of this one identified the "Entanglement-ring" (E-ring) with diameter $D = 2\alpha F$. Each couple of points symmetrically opposed through the center of the E-ring were then correlated by quantum entanglement. An annular mask with diameter $D = 1.5\text{cm}$ and width $\delta = .1\text{cm}$ provided an accurate spatial selection of the E-ring and an efficient filtering of the unwanted UV light out of the measurement apparatus. The E-ring spatial photon distribution was divided in two equal portions along a vertical axis by a prism-like, two-mirror system and collected by two lenses that focused all the radiation on the active cathodes of two independent measurement devices at sites \mathcal{A} and \mathcal{B} : *Alice* and *Bob*. Optionally, two optical fibers could convey the radiation to two far apart stations, \mathcal{A} and \mathcal{B} . The indices 1 and 2 will also be adopted henceforth to identify local quantities as angles, states etc. measured in spaces \mathcal{A} and \mathcal{B} , respectively. The radiation reaching sites \mathcal{A} and \mathcal{B} was detected by two Si-APD photodiodes SPCM-AQR14, with $DQE = 65\%$ and dark count rate $\simeq 50\text{s}^{-1}$. Typically, two equal interference filters (IF) were placed in front of the \mathcal{A} and \mathcal{B} detectors. The bandwidth $\Delta\lambda_j = 6\text{nm}$ of the two IF's determined the *coherency thickness* δ of the cylindrical distribution and the *coherence-time* of the emitted photons: $\tau_{coh} \approx 140$ femtoseconds. The simultaneous detection of the *whole ensemble* of the SPDC emitted entangled pairs allowed a quantitative assesment of the absolute *brightness* of

the source. The UV pump power adopted in the experiment was: $P_p \simeq 40mW$. At such a low power typically 4000 coincidences per second were detected, thus outperforming by an order at least 10^3 the overall *quantum efficiency* of the common SPDC sources [5]. On the other hand in these conditions the NL parametric gain was so small, $g < 10^{-3}$ that the ratio of the probabilities for simultaneous *stimulated-emission* of two i^{th} -pairs and the one for the *spontaneous-emission* of one i^{th} -pair was $< 10^{-6}$.

The present demonstration was carried out in the λ -degenerate condition, i.e. the highest probability process, according to NL Optics. Note however that the apparatus works perfectly for a very general λ -*non-degenerate* dynamics, i.e. by allowing at the extreme the *simultaneous* detection, by sufficiently broadband detectors, of the *full set* of SPDC generated i^{th} -pairs with all possible phase-matching allowed combinations of wl's λ_{ji} , $j = 1, 2$.

Note the high structural flexibility of this novel SPDC source. Its structure indeed suggests the actual implementation of several relevant schemes of quantum information and communication, including entanglement multiplexing, joint entanglement over $\vec{\pi}$ and k -vector degrees of freedom etc. Furthermore, it also suggests the realization of a confocal cavity Optical Parametric Oscillator emitting a non-thermal, E-ring distribution of entangled photon states. These ideas are presently being investigated in our laboratory.

Violation of Bell inequalities by a pure state: The Bell state expressed by Eq. 1 with $\phi = \pi$, i.e. a "singlet" over the whole *E-ring* was adopted to test the violation of a Bell inequality by the standard coincidence technique [3,15]. The adopted angle orientations of the $\vec{\pi}$ -analyzers located at the \mathcal{A} (1) and \mathcal{B} (2) sites were:

$\{\theta_1 = 0, \theta'_1 = \pi/2\}$ and $\{\theta_2 = \pi/4, \theta'_2 = 3\pi/4\}$, together with the respective orthogonal angles: $\{\theta_1^\perp, \theta'^\perp_1\}$ and $\{\theta_2^\perp, \theta'^\perp_2\}$. By these values, the standard Bell-inequality parameter could be evaluated [3,7]:

$S = |P(\theta_1, \theta_2) - P(\theta_1, \theta'_2) + P(\theta'_1, \theta_2) + P(\theta'_1, \theta'_2)|$ where:

$P(\theta_1, \theta_2) = [C(\theta_1, \theta_2) + C(\theta_1^\perp, \theta_2^\perp) - C(\theta_1, \theta_2^\perp) - C(\theta_1^\perp, \theta_2)] \times$

$[C(\theta_1, \theta_2) + C(\theta_1^\perp, \theta_2^\perp) + C(\theta_1, \theta_2^\perp) + C(\theta_1^\perp, \theta_2)]^{-1}$ and $C(\theta_1, \theta_2)$ is the coincidence rate

measured at sites \mathcal{A} and \mathcal{B} . Fig.2 shows the $\vec{\pi}$ -correlation pattern obtained by varying

the angle θ_1 of the \mathcal{B} analyzer in the range ($45^\circ - 135^\circ$), having kept fixed the angle of the \mathcal{A} analyzer : $\theta_2 = 45^\circ$. The dotted line expresses in Fig.2 the limit boundary between the quantum and the "classical" regimes. The measured value $S = 2.5564 \pm .0026$, obtained by integrating the data over 180s, corresponds to a violation as large as 213 standard deviations respect to the limit value $S = 2$ implied by *local realistic* theories [7]. A very small amount of noise appears to affect in Fig.2 the experimental data which also fit well the theoretical (continuous) curve expressing the *ideal* interferometric pattern with maximum *visibility*: $V = 1$. In addition to its remarkable conceptual relevance because of the adoption of a *pure-state*, this result expresses the good overall performance of our optical system including the accuracy obtainable for the optical superposition and focusing of large beams. The good performance was, of course also attributable due to the *high brightness* of the source. In facts, owing to $SQE \approx 1$, a large set of statistical data could be accumulated in exceedingly short measurement times and with very low UV pump powers.

Generation and characterization of Werner states. Because of the peculiar spatial superposition property of the output state, the present apparatus appears to be an ideal source of *any* bi-partite, two-qubit entangled state, either *pure* or *mixed*. In particular of the Werner state: $\rho_W = p|\Psi_-\rangle\langle\Psi_-| + \frac{1-p}{4}\mathbf{I}$ consisting of a mixture of a *pure* singlet state $|\Psi_-\rangle = 2^{-\frac{1}{2}}\{|HV\rangle - |VH\rangle\}$ with probability p ($0 \leq p \leq 1$) and of a fully *mixed-state* expressed by the unit operator \mathbf{I} . The corresponding density matrix, expressed in the basis $|HH\rangle, |HV\rangle, |VH\rangle, |VV\rangle$ is:

$$\rho_W = \begin{pmatrix} A & 0 & 0 & 0 \\ 0 & B & C & 0 \\ 0 & C & B & 0 \\ 0 & 0 & 0 & D \end{pmatrix} \quad (2)$$

with: $A=D=\frac{1}{4}(1-p)$, $B=\frac{1}{4}(1+p)$, $C=-p/2$. The Werner states possess a highly conceptual and historical value because, in the probability range $[1/3 < p < 1/\sqrt{2}]$, they *do not* violate any Bell's inequality in spite of being in this range *nonseparable* entangled states,

precisely *NPT states* [11].

How to synthesize by our source these paradigmatic, utterly remarkable states ?

Among many possible alternatives, we selected a convenient *patchwork* technique implying the following steps: **[1]** Making reference to the original *source-state* expressed by Eq.1, a *singlet state* $|\Psi_{-}\rangle$ was easily obtained by inserting a $\vec{\pi}$ -*flipping*, zero-order $\lambda/2$ wp in front of detector \mathcal{B} . **[2]** A anti-reflection coated glass-plate G , $200\mu\text{m}$ thick, inserted in the d – *section* with a variable trasverse position Δx , introduced a decohering fixed time-delay $\Delta t > \tau_{coh}$ that spoiled the *indistinguishability* of the *intercepted portions* of the overlapping *quantum-interfering* radiation cones: Fig.3, inset. As a consequence, *all non-diagonal* elements of ρ_W contributed by the surface sectors $\mathbf{B} + \mathbf{C}$ of the E-ring, the ones optically intercepted by G , were set to *zero* while the non intercepted sector \mathbf{A} expressed the *pure-state* singlet contribution to ρ_W . **[3]** A $\lambda/2$ wp was inserted in the semi-cylindrical photon distribution reflected by the beam-splitting prism towards the detector \mathcal{A} . Its position was carefully adjusted in order to intercepts *half* of the $\mathbf{B} + \mathbf{C}$ sector, i.e. by making $\mathbf{B} = \mathbf{C}$. Note that only *half* of the E-ring needed to be intercepted by the optical plates, in virtue of the EPR nonlocality. The other, optically non-intercepted, half of the E-ring is not represented in Fig.3, inset. In summary, the sector \mathbf{A} of the E-ring contributed to ρ_W with a *pure state* $p|\Psi_{-}\rangle\langle\Psi_{-}|$, the sector $\mathbf{B} + \mathbf{C} = 2\mathbf{B}$ with the *statistical mixture*: $\frac{1-p}{4} \{ [|HV\rangle\langle HV| + |VH\rangle\langle VH|] + [|HH\rangle\langle HH| + |VV\rangle\langle VV|] \}$ and the probability p , a monotonic function of Δx , could be easily varied over its full range of values: $p \propto \Delta x$ for small p . The two extreme cases are: **[a]** The G and the $\lambda/2$ wp intercepting the beam towards \mathcal{A} are absent: $\mathbf{B} = \mathbf{C} = 0$. The A section covers *half* of the E-ring and: $\rho_W \equiv |\Psi_{-}\rangle\langle\Psi_{-}|$; **[b]** The G plate intercepts *half* of the E-ring and the position of the $\lambda/2$ wp intercepting the beam towards \mathcal{A} is set to make $\mathbf{B} = \mathbf{C}$. In this case $\mathbf{A} = 0$ and: $\rho_W \equiv \frac{1}{4}\mathbf{I}$. Optionally, the setting of the $\lambda/2$ wp intercepting the beam towards \mathcal{A} could be automatically activated by the *single* setting Δx , e.g. via an electromechanical servo.

Any Werner state could be realized by this technique, by setting $\mathbf{B} = \mathbf{C}$ and by adjusting the value of $p(\Delta x)$. Far more generally, *all possible* bi-partite states in 2×2 dimensions

could be created by this technique. This indeed expresses the "universality" of our source.

A set of Werner states was indeed synthesized and several relevant properties investigated by our method leading to the experimental results shown in Fig 3 and 4a). A relevant property of any mixed-state, the "tangle" $T = [C(\rho)]^2$, i.e. the square of the *concurrence* $C(\rho)$, is directly related to the *entanglement of formation* $E_F(\rho)$ and expresses the degree of entanglement of ρ [16]. Another important property of the mixed-states is the "linear entropy" $S_L = d(1 - \text{Tr}\rho^2)/(d - 1)$, $S_L = (1 - p^2)$ for Werner states, which quantifies the degree of disorder, viz. the *mixedness* of a system with dimensions d [17]. In virtue of the very definition of $C(\rho)$, these two quantities are found to be related, for Werner states, as follows: $T_W(S_L) = \frac{1}{4}(1 - 3\sqrt{1 - S_L})^2$ for $0 \leq S_L \leq 8/9$ [16]. As shown in Fig.3, for S_L in the range $[\frac{1}{2} \leq S_L \leq 8/9]$ the Bell inequalities are not violated while ρ_W is a *separable*, PPT state for $S_L > 8/9$ and $T(S_L) = 0$ [11]. The experimental result shown in Fig.4a of a standard tomographic analysis of the Werner state corresponding to $p \simeq 0.42$ reproduces graphically, and quite accurately the structure of the matrix ρ_W expressed by Eq.2. The properties $T_W(S_L)$ of a full set of Werner states are also reported in Fig. 3. There the experimental points (full circles) are determined according to the following procedure. First, the position Δx of the plate G is set according to a pre-determined, zeroth-order value of p . Then, a tomographic experiment reproducing a result similar to Fig. 4a and a numerical optimization procedure lead to the determination of the *actual* value of ρ , $\text{Tr}\rho^2$ and then of S_L . It leads to the *actual* value of p , p_{sp} [18]. Finally, ρ is adopted to evaluate the *actual* value of $T_W = [C(\rho)]^2$. We may check in Fig.3 the good agreement of the experimental data with the theoretical result expressed by the plotted function $T_W(S_L)$. The state represented by Fig.4a, and also reproduced in Fig.3, *does not* violate any Bell inequality, in spite of being a *non separable* one. Indeed, the corresponding Bell-inequality parameter has been experimentally measured: $S = 1.048 \pm 0.011$. The transition to $S > 2$ has been experimentally determined, and found consistent with theory, by increasing the value of p in order to set $S_L = (1 - p^2) < \frac{1}{2}$.

Generation and characterization of MEMS states. As a final demonstration

of the universality of our method, a full set of "maximally entangled mixed states" (MEMS) was synthesized by our source and tested again by quantum tomography [14,18]. To the best of our knowledge, a similar result was not previously reported in the literature. On the other hand, according to the introductory notes expressed above, the MEMS are to be considered, for *practical* reasons, as important resources of modern QI because they achieve the *greatest possible* entanglement for a given mixedness, i.e. the one which is the unavoidable manifestation of *decoherence*. Of course, in order to synthesize the MEMS a convenient partition of the *E-ring*, different from the one shown in Fig.3, has been adopted. The class of MEMS generated and tested by our method are expressed by ρ_{MEMS} which is again given in matrix form by Eq. 2, with the following parameters: $A=(1-2g(p))$, $B=g(p)$, $C=-p/2$, $D=0$ and: $g(p) = p/2$ for $p \geq 2/3$ and $g(p) = 1/3$ for $p < 2/3$. The tomographic result shown in Fig.4b reproduces graphically, and with fair accuracy the ρ_{MEMS} structure with the parameter: $p = 0.56$ and then: $g(p) = 1/3$. However, the agreement between experimental and theoretical results expressed in Fig.3 is less satisfactory for MEMS than it was for Werner states. This is due to the strict experimental requirements implied by the tricky realization of these exotic objects. Improvements in this direction as well as investigations with the new source in related domains of quantum information are presently being tackled in our laboratory [19].

Thanks are due to W.Von Klitzing for useful discussions and early involvement in the experiment. This work was supported by the FET European Network on Quantum Information and Communication (Contract IST-2000-29681: ATESIT) and by PRA-INFN 2002 (CLON).

REFERENCES

- [1] E. Schroedinger, 1935, *Proc. Cambridge Phil. Soc.* 31, 555.
- [2] L. Rosenfeld, Commentary to EPR (1967) in: *Quantum Theory and Measurement* (J.A. Wheeler and W.H. Zurek eds., Princeton U. Press, 1983).
- [3] J. S. Bell, *Speakable and Unsayable in Quantum Mechanics* (Cambridge University Press, 1988); A. Aspect, P. Grangier and G. Roger, *Phys. Rev. Lett.* 49, 91 (1982); M. Jammer, *The Philosophy of Quantum Mechanics* (Wiley, New York, 1974).
- [4] E. S. Fry, T. Walther and S. Li, *Phys. Rev. A*, 52, 4381 (1995).
- [5] D. Klyshko, *Photons and Nonlinear Optics* (Gordon and Breach, New York, 1988); P. G. Kwiat, K. Mattle, H. Weinfurter and A. Zeilinger, A. V. Sergienko, Y. Shih, *Phys. Rev. Lett.* 75, 4337 (1995); D. Boschi, F. De Martini and G. Di Giuseppe, 1998, *Fortschritte der Physik* 46, 643 (1998).
- [6] Alain Aspect, private communication to F. D. M.
- [7] J. F. Clauser, M. A. Horne, A. Shimony and R. A. Holt, *Phys. Rev. Lett.* 23, 880 (1969); E. Santos, *ibid.* 66,1388 (1991) N.D. Mermin, in *New Techniques and Ideas in Quantum Measurement* (The N.Y.Academy of Sciences, New York, 1986); A. Garuccio, *Phys.Rev.A*, 52, 2535 (1995).
- [8] J. F. Clauser and M. A. Horne, *Phys. Rev. D* 10, 526 (1974).
- [9] C. H. Bennett and S. J. Wiesner, *Phys. Rev. Lett.* 69, 2881(1992).
- [10] C. H. Bennett, G. Brassard, C. Crepeau, R. Jozsa, A. Peres and W. K. Wootters, *Phys. Rev. Lett.* 70, 1895 (1993); D. Boschi, S. Branca, F. De Martini, L. Hardy and S. Popescu, *ibid.* 80, 1121 (1998); D. Bouwmeester, J. M. Pan, K. Mattle, M. Eibl, H. Weinfurter and A. Zeilinger, *Nature (London)* 390, 575 (1997).
- [11] A. Peres, *Phys. Rev. Lett.* 77, 1413 (1996); M. Lewenstein, D. Bruss, J.I. Cirac, B.

- Kraus, M. Kus, J. Samsonowicz, A. Sampera and R. Tarrach, *Journal of Modern Optics*, 47, 2841 (2000); M. Horodecki, P. Horodecki and R. Horodecki, in: *Quantum Information: An Introduction to Basic Theoretical Concepts and Experiments* (Springer, Berlin 2001); D. Bruss, J.I. Cirac, P. Horodecki, F. Hulpke, B. Kraus and M. Lewenstein, *Journ. of Mod. Optics*, 49, 1399 (2002).
- [12] M. Horodecki, P. Horodecki and R. Horodecki, *Phys. Rev. Lett.* 80, 5239 (1998).
- [13] R. F. Werner, *Phys. Rev. A* 40, 4277 (1989).
- [14] S. Ishizaka, T. Hiroshima, *Phys. Rev. A*, 62, 022310 (2000), W. J. Munro, D. F. V. James, A.G. White and P. G. Kwiat, *ibid.* 64, 030302 (2001), F. Verstraete, K. Audenaert and B. De Moor, *ibid.* 64, 012316 (2001).
- [15] Y. H. Shih and C. O. Alley, *Phys. Rev. Lett.* 61, 2921 (1988); Z. Y. Ou and L. Mandel, *ibid.* 61, 50 (1988); P. G. Kwiat, K. Mattle, H. Weinfurter, A. Zeilinger, A. V. Sergienko and Y. Shih, *ibid.* 75, 4337 (1995).
- [16] W. K. Wootters, *Phys. Rev. Lett.* 80, 2245, (1998); S. Bose and V. Vedral, *Phys. Rev. A*. 61, 040101(2000); V. Coffman, J. Kundu, W. K. Wootters, *ibid.* 61, 052306 (2000). Since $E_F(\rho)$, $C(\rho)$, T are monotonic functions of one another, they are equivalent measures of entanglement.
- [17] A.G. White, D. F. V. James, W. J. Munro and P. G. Kwiat, *Phys. Rev. A*. 65, 012301(2001); Yong-Sheng Zhang, Yun-Feng Huang, Chuan-Feng Li and Guang-Can Guo, *ibid.* 66, 062315 (2002).
- [18] D. F. V. James, P. G. Kwiat, W. J. Munro and A.G. White, *Phys. Rev. A*. 64, 052312 (2001).
- [19] G. Giorgi, G. Di Nepi, P. Mataloni and F. De Martini, *Laser Physics*, 13-3 (2003).

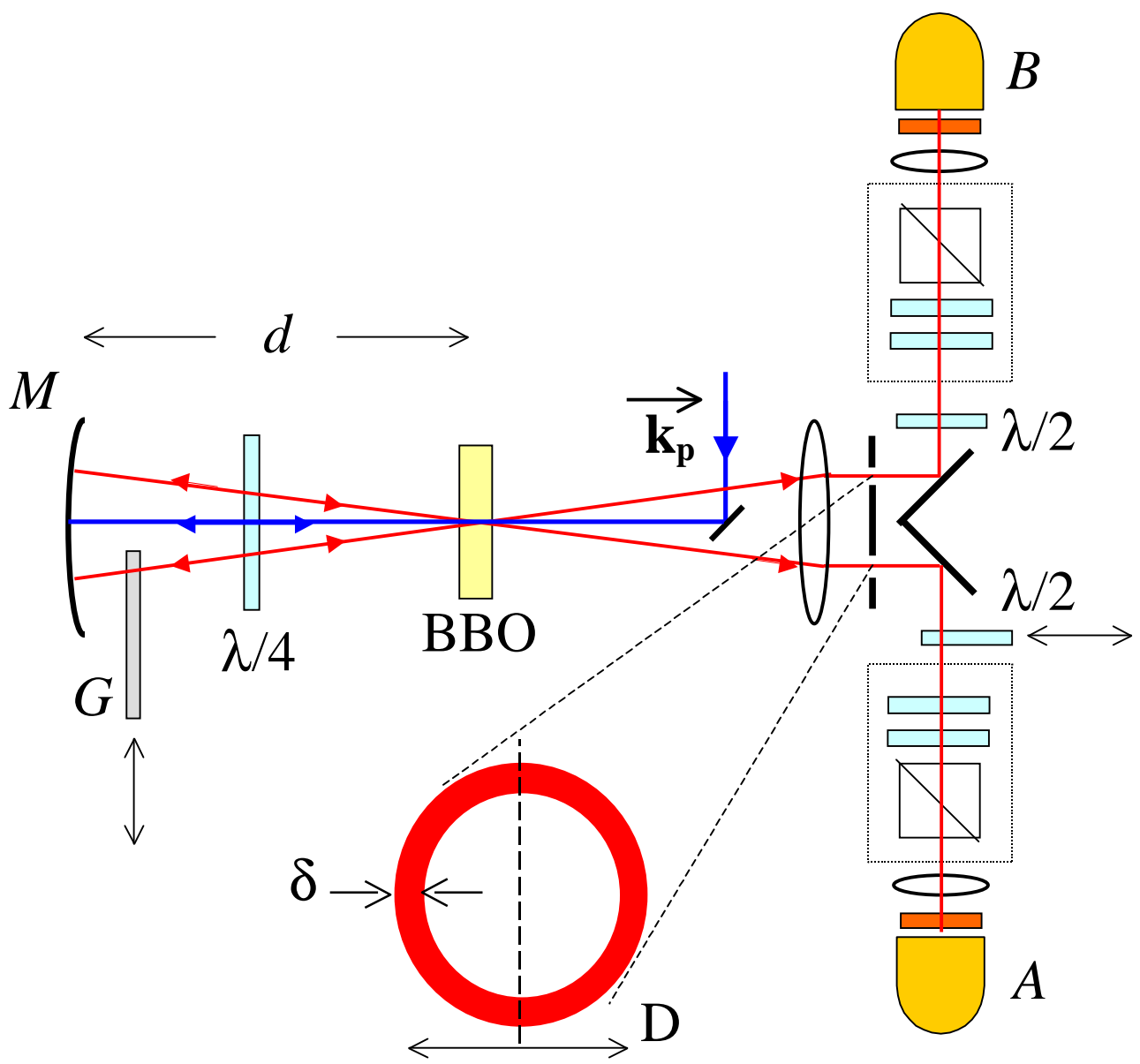
Figure Captions

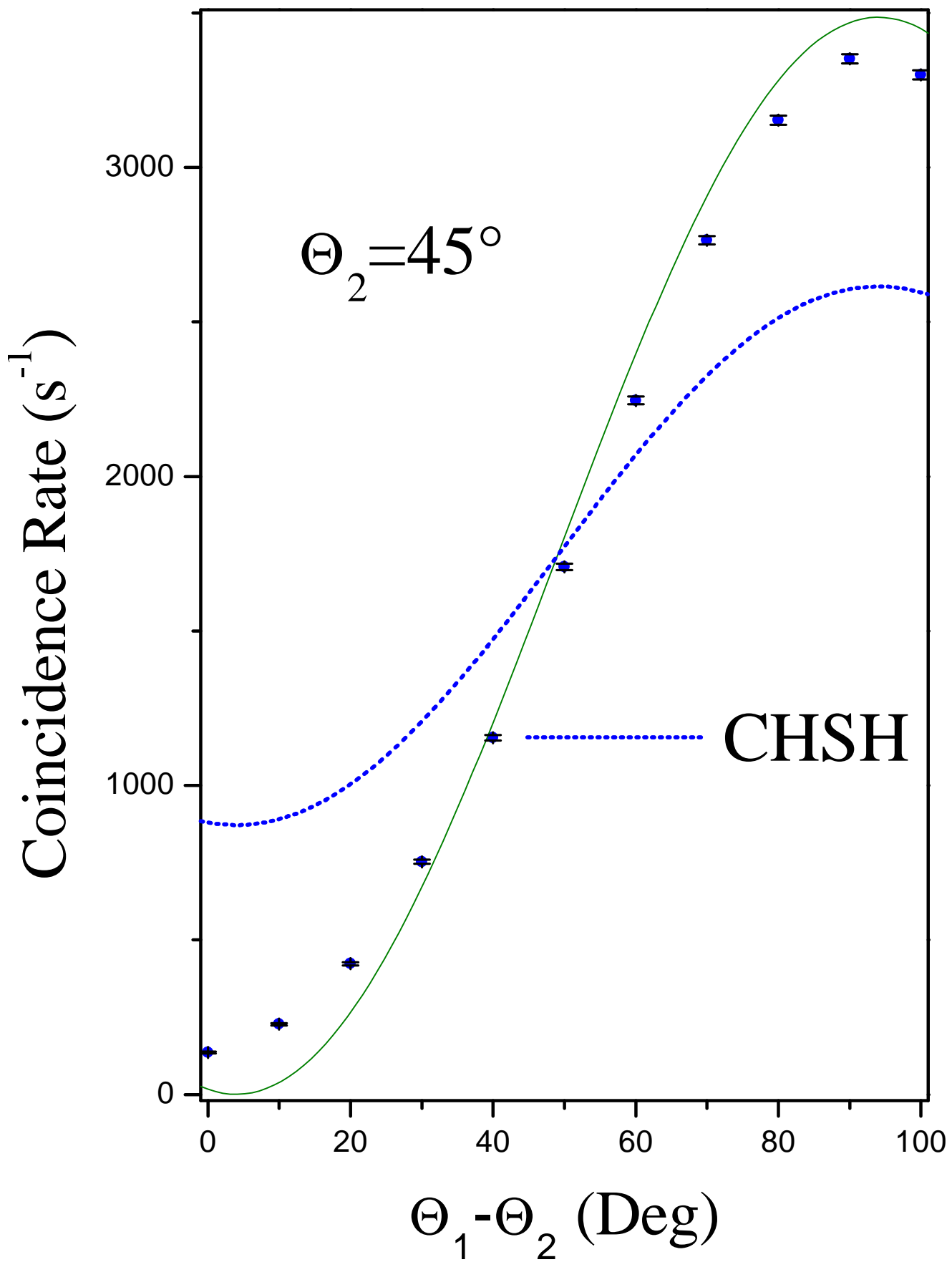
Figure 1: Layout of the *universal, high-brightness* source of polarization ($\vec{\pi}$) entangled *pure-states* and of general *mixed-states* of photons.

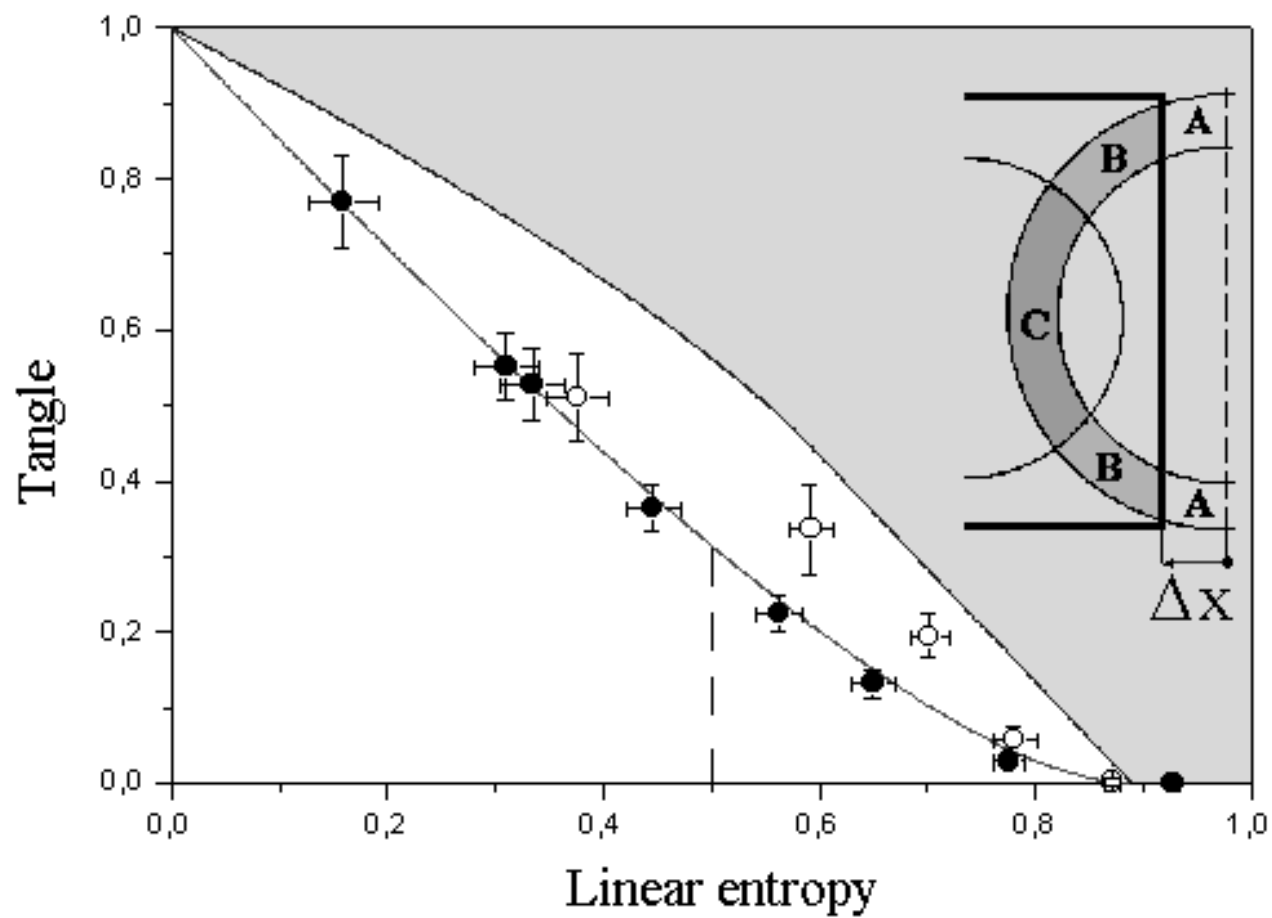
Figure 2: Violation of a Bell Inequality by a "singlet" *pure-state*. The *dotted* curve expresses the transition between standard quantum theory and *local realistic theories*. The *continuous* curve expresses the *optimal* theoretical behavior with interferometric visibility: $V = 1$. The statistical noise of each experimental datum is expressed by the corresponding error flag.

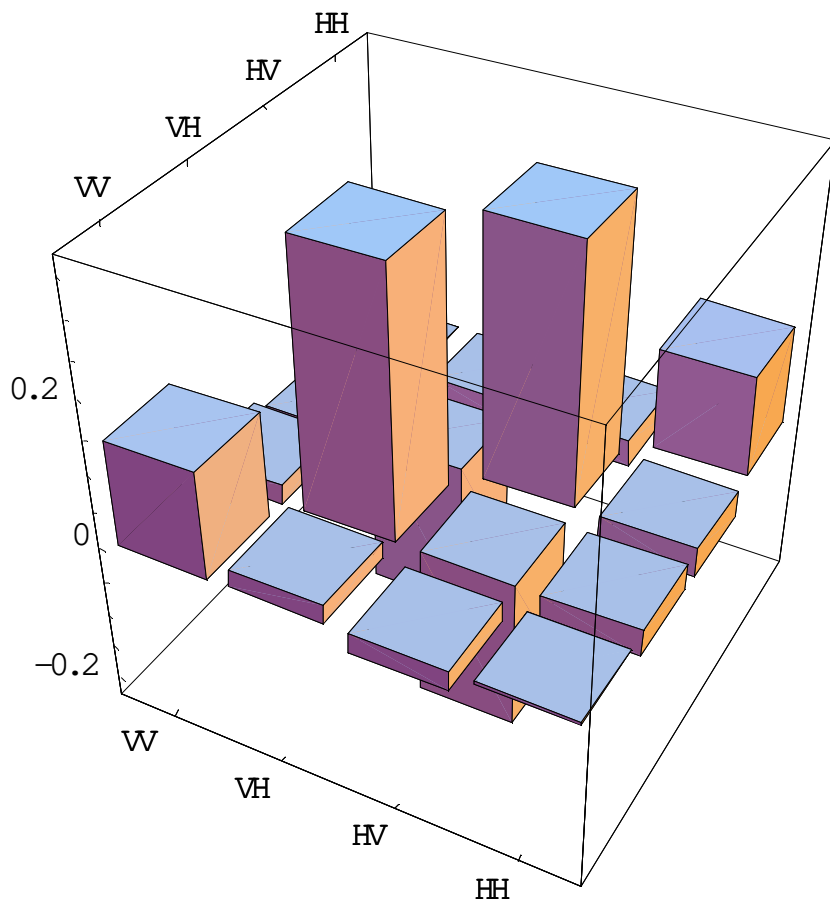
Figure 3: Experimental plots of the "Tangle" T vs the "Linear entropy" S_L for Werner states (full circles) and *maximum-entangled-mixed-states* (MEMS) (open circles). The vertical dotted line expresses the boundary between the two regimes corresponding to non-separable states violating and non-violating Bell inequalities. The shaded region on the upper right side is dynamically inaccessible. INSET: Partition of the (half) *Entanglement-ring* into the spatial contributions of the emitted entangled-pair distribution to an overall output Werner-state.

Figure 4: Experimental quantum tomographic reconstructions of: (a) A Werner-state ρ_W with "singlet" probability $p = 0.42$ and: (b) A MEMS-state ρ_{MEMS} with $p = 0.56$. The two tomographic patterns reproduce graphically the structure of the ρ -matrix expressed by Eq. 2 with the appropriate parameters.

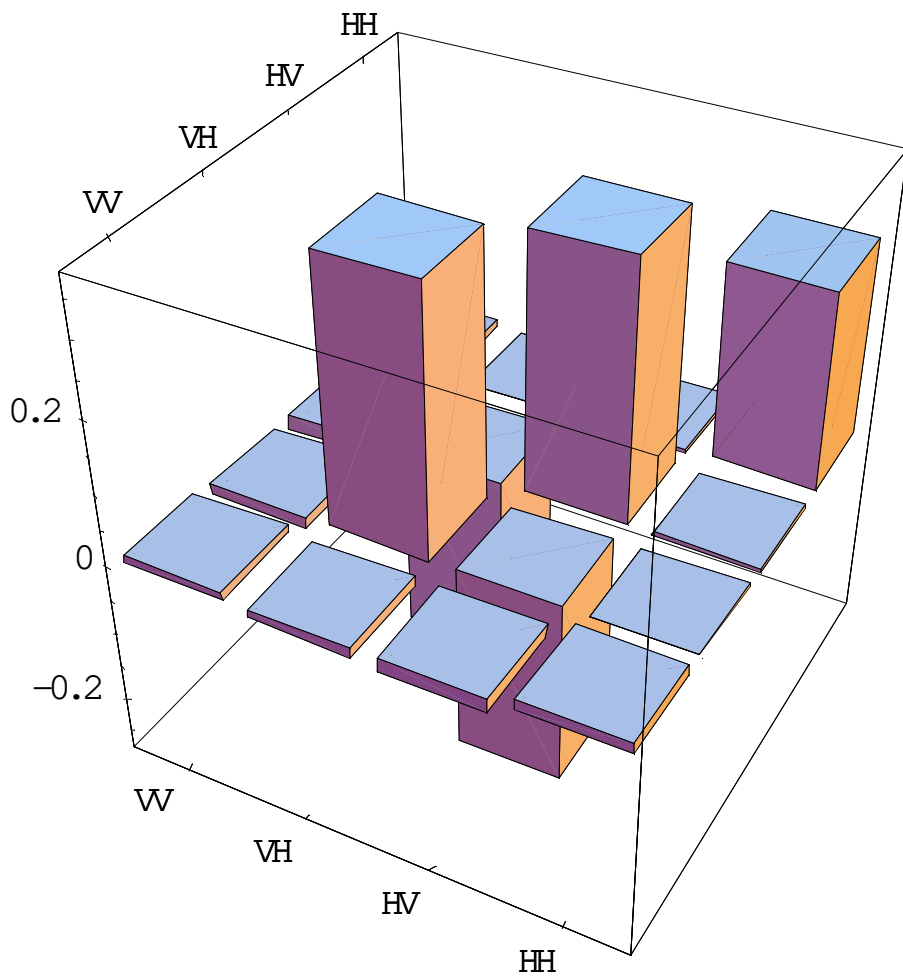








a)



b)